Pis'ma v ZhETF, vol.64, iss.3, pp.178 - 182 © 1996 August 10

OBSERVATION OF A RADIATION-INDUCED SOLITON RESONANCE IN A JOSEPHSON RING

A. V. Ustinov

Institute of Thin Film and Ion Technology, Research Center (KFA)
D-52425 Jülich, Germany

Institute of Solid State Physics RAS
142432 Chernogolovka, Moscow district, Russia

Submitted 4 July 1996

Experimental study of single-soliton dynamics in a ring-shaped Josephson junction is reported. An externally applied magnetic field H forms a harmonic potential for the soliton in the ring. Rotation of the soliton in the junction leads to a potential-induced emission of plasma waves which give rise to a resonance at a certain soliton velocity. This behavior agrees with numerical simulations which indicate locking of the soliton to the radiation frequency. Good agreement between experiment, kinematic model and numerical simulations is found.

PACS: 03.40.Kf, 03.65.Pm, 74.50.+r

Motion of a sine-Gordon soliton in a spatially periodic potential has been studied in several theoretical papers rather long time ago [1, 2]. It has been shown that the soliton radiates small-amplitude waves with plasma dispersion relation. The wave frequency depends on the soliton velocity and the period of the potential [2]. A fluxon (a Josephson vortex carrying one magnetic flux quantum Φ_0) in a long Josephson junction is a well known example of a soliton described by the perturbed sine-Gordon model. It has been predicted [3] that in a periodically-modulated junction of the finite length ℓ the generated radiation should lead to resonances which appear as additional steps on a current-voltage ($I-V$) characteristics. These resonances have been observed in experiments [4] using an artificially prepared lattice of inhomogeneities in the junction. Such a realisation of the periodic potential appears to be rather straightforward but it does not allow to control the potential amplitude and its shape during the experiment.

Ring-shaped (annular) long Josephson junctions serve as the best model objects for studying soliton dynamics. Due to the magnetic flux quantization in a superconducting ring, the number of fluxons initially trapped in an annular junction is conserved. The fluxon dynamics can be studied here under periodic boundary conditions. While the fabrication of annular Josephson tunnel junctions is rather easy, trapping of fluxons in them remains the state of art. Using different trapping techniques, both single-fluxon [5] and multi-fluxon [6] dynamics have been investigated in homogeneous annular junctions.

In this letter I present experiments with a single fluxon trapped in an annular Josephson junction which is placed in the an externally applied magnetic field H. The geometry is schematically shown in Fig.1. Due to the interaction of the fluxon with the radial field component, the fluxon moves in a harmonic potential $U(\theta) \sim U_0 \cos\theta$ with the amplitude U_0 proportional to H. The minimum of the potential is located in the region of the ring where the fluxon is directed along the field. The theoretical model for this system was proposed by Grønbech-Jensen et al. [7]. The field accounts for an additional term in the perturbed sine-Gordon equation which describes the fluxon motion:

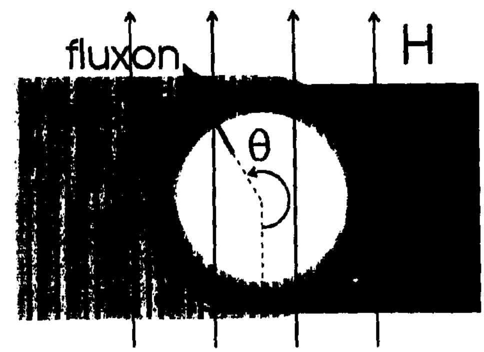

Fig.1. Schematic view of an annular junction with trapped fluxon; a magnetic field H is applied in the plane of the tunnel barrier

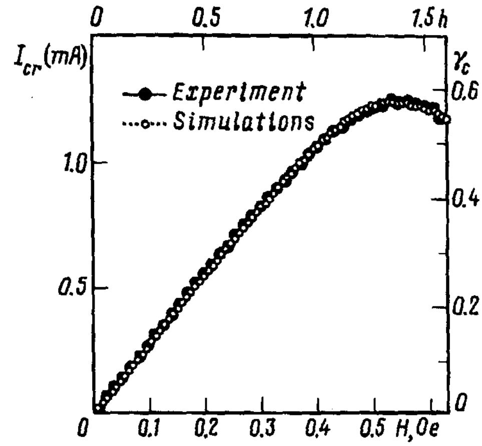

Fig.2. The critical current I_{cr} of the annular junction with one trapped fluxon versus the applied magnetic field H. Simulations of $\gamma_{cr}(h)$ were performed by numerical integration of Eq. (1)

$$\varphi_{xx} - \varphi_{tt} = \sin\varphi + \alpha\varphi_t - \gamma - h\sin\frac{2\pi x}{\ell}, \tag{1}$$

where $\varphi(x,t)$ is a superconducting phase difference between the electrodes of the junction, the spatial coordinate x along the ring is normalized to the Josephson penetration depth λ_J, the time t is normalized to the inverse plasma frequency ω_0^{-1}, α is the dissipation coefficient due to the quasiparticle tunnelling across the barrier, γ is the bias current density normalized to the critical current density J_c of the junction, and $\ell = \pi D/\lambda_J$, D being the ring's diameter. The last term in Eq. (1) accounts for the coupling between the applied field and the flux density in the junction. The dimensionless amplitude $h \propto H$ is normalized by a sample-specific geometrical factor [7, 8]. In case of one fluxon trapped in the ring, Eq. (1) is supplemented by the periodic boundary condition $\varphi(\ell) = \varphi(0) + 2\pi$. At low velocities the fluxon's coordinate is described by the equation which is similar to that of a driven pendulum in a lossy medium [9].

Experiments have been performed on Nb/Al-AlO_x/Nb Josephson junctions. Trapping of a magnetic flux in the ring was made while cooling the sample below the critical temperature $T_c^{Nb} = 9.2\,K$ of niobium with a small bias current passing through the junction. Measurements were performed by applying the bias current I from top to the bottom electrode of the junction and measuring the dc voltage generated due to the fluxon motion. Results presented below were obtained for a junction with the mean diameter $D = 132\,\mu m$ and the ring width $W = 10\,\mu m$. The normalized ring's circumference at $T = 7.3\,K$ was estimated $\ell \approx 7.7$.

Fig.2 shows the measured and numerically simulated critical current I_{cr} of the annular junction with one trapped fluxon versus the applied magnetic field H. At $H = 0$ the zero-voltage depinning current I_{cr} is very small, by a factor of about

300 smaller than the critical current I_c measured for the same junction without trapped fluxon. This indicates the very high homogeneity of the junction. The linear increase of I_{cr} at low fields is well described by the theoretical model [7] based on Eq. (1). The zero-voltage state is stable as long as the maximum pinning force due to the field-induced potential is larger than the bias current force acting on the fluxon. This is satisfied in the range $|\gamma| < \gamma_{cr}$ where $\gamma_{cr} = h\,\mathrm{sech}(\pi^2/\ell)$ [7]. The nonlinear region of $I_{cr}(H)$ at high fields has been recently studied by Vernik et al. [10]. The fluxon $I-V$ characteristics in the low field range are shown in Fig.3. As indicated on the plot, four presented curves correspond to different values of H. At $H \neq 0$ the current I_{cr} increases and hysteresis appears on the $I-V$ curve. At $I > I_{cr}$ the fluxon overcomes the pinning potential and starts to move in the junction, thereby generating a dc voltage. If the bias current is decreasing, the underdamped fluxon motion continues until the current is low enough for the fluxon to be trapped by the well.

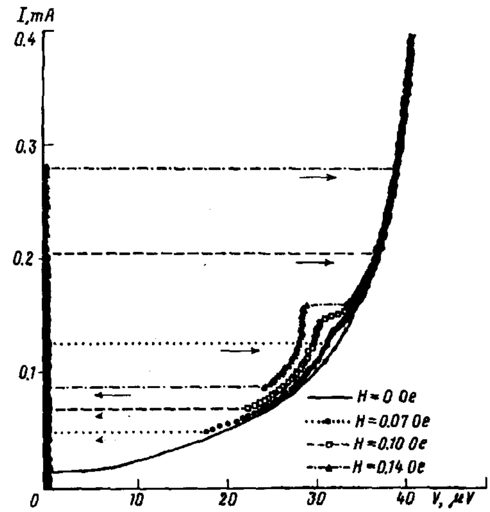

Fig.3. Current-voltage characteristics of a single fluxon rotating in the junction at $T = 7.3$ K. Different applied magnetic fields H are indicated on the plot. Horizontal arrows show switching directions

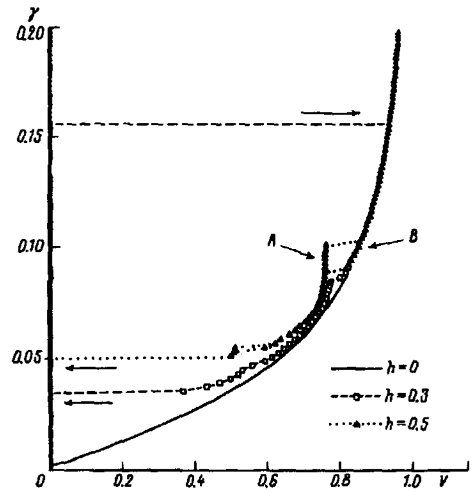

Fig.4. Numerically simulated current-voltage characteristics of a single fluxon for junction parameters $\ell = 7.8$, $\alpha = 0.05$ and h as indicated on the plot. The resonant step associated with the fluxon interaction with its radiation is seen at $v \approx 0.75$

The $I-V$ characteristics presented in Fig.3 show a clear resonant step at $28-30\,\mu$V. With increasing H, the $I-V$ curve first shows a small bump at about $30\,\mu$V which evolves at higher fields in a pronounced step. At fixed H, the shape of this step is strongly dependent on the temperature. We have simulated the current-voltage curves (bias current γ vs the fluxon velocity v) by numerically integrating Eq. (1). The simulation results with parameters $\ell = 7.8$ and $\alpha = 0.05$, close to that in experiment, are presented in Fig.4. One can see that the qualitative agreement between the simulations and the experimental data of Fig.3 is very good. Some features of the internal dynamics of the junction corresponding to the simulated $\gamma(v)$ characteristics are shown in Fig.5. One can see that the resonant step at $v \approx 0.75$ is characterized by the background voltage oscillations (plasma waves) with a period in time, which is 3 times smaller than the fluxon oscillation period. Thus, at sufficiently large h the fluxon strongly interacts with the field-induced potential and a large part of its energy is transferred into the radiation.

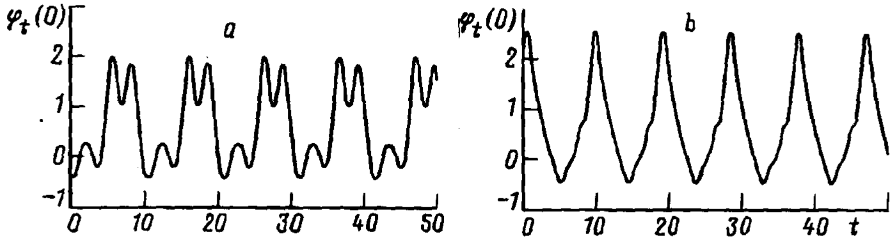

Fig.5. Voltage oscillations at $x = 0$ for two different points of the $\gamma(v)$ curve with $h = 0.5$ shown in Fig.4: (a) at the radiation-induced step, point **A** ($\gamma = 0.09$, $v = 0.75$); (b) at the main fluxon step, point **B** ($\gamma = 0.10$, $v = 0.84$)

A simple model for the potential-induced fluxon radiation can be proposed in the following way. A fluxon rotating in an annular junction can be viewed as moving in a periodic potential which has a spatial period of ℓ. Under such conditions, the fluxon is predicted to emit small-amplitude plasma waves, the wavenumber k and frequency $\omega = \sqrt{1+k^2}$ of which depend on the period ℓ and the fluxon velocity v [2]. The radiation should lead to a series of resonances at $\omega = 2\pi nv/\ell$, where n is an integer. These resonances where predicted [3, 11] to appear as steps on $I - V$ characteristics at the fluxon velocities

$$v_n = \sqrt{\left(1 - \frac{L}{na}\right)^2 + \left(\frac{L}{2\pi n}\right)^2}, \tag{2}$$

where L is the spatial period of fluxon oscillations and a is the period of the potential. According to Mkrtchyan and Schmidt [2], the amplitude of the emitted waves is the highest near the radiation threshold $v_{\text{thr}} = \left[1 + (2\pi/L)^2\right]^{-1/2}$. Using Eq. (2) with $L = a = \ell = 7.8$, we obtain $v_3 \approx 0.785$ to be the closest resonance to the threshold velocity $v_{\text{thr}} \approx 0.779$. This prediction is in good agreement with experimentally measured (Fig.3) and theoretically calculated (Fig.4) position of the resonance step. Moreover, the radiation frequency in Fig.5(a) corresponds to $n = 3$, as expected.

At low temperatures the radiation step becomes more complicated in shape, showing negative differential resistance and chaotic switching between several closely located branches. For low losses, such a complex resonance was earlier simulated numerically [9] and has been attributed to a strong fluxon-plasma wave interaction leading to an intrinsically chaotic dynamics in the junction. Though the background oscillations were discussed, the authors of [9] did not suggest any analytical model which can predict the voltage of the resonance or the harmonic number n. From the model presented above it can be argued that chaos in this system is possible due to a competition between several resonances lying at close voltages. For example, $n = 2$ and $n = 4$ resonances predicted by Eq. (2) occur at $v_2 \approx 0.797$ and

$v_4 \approx 0.812$. Thus, reduction of losses (decrease of temperature) can be expected to complicate the dynamics, as indeed was observed experimentally. A more detailed investigation of these effects will be published elsewhere.

I would like to thank N.Thyssen for sample fabrication and B.A.Malomed for useful discussions.

---

1. D.W.McLaughlin and A.C.Scott, Phys. Rev. A **18**, 1652 (1978).
2. G.S.Mkrtchyan and V.V.Schmidt, Solid St. Commun. **30**, 791 (1979).
3. A.A.Golubov and A.V.Ustinov, IEEE Trans. Magn. **23**, 781 (1987).
4. I.L.Serpuchenko and A.V.Ustinov, Pis'ma ZhETF **46**, 435 (1987) [Sov. Phys. JETP Lett. **46**, 549 (1987)].
5. A.Davidson, B.Dueholm, B.Kryger, and N.F.Pedersen, Phys. Rev. Lett. **55**, 2059 (1985).
6. A.V.Ustinov, T.Doderer, R.P.Huebener et al., Phys. Rev. Lett. **69**, 1815 (1992).
7. N.Grønbech-Jensen, P.S.Lomdahl, and M.R.Samuelsen, Phys. Lett. A **154**, 14 (1991).
8. N.Martucciello and R.Monaco, Phys. Rev. B **53**, 3471 (1996).
9. N.Grønbech-Jensen, P.S.Lomdahl, and M.R.Samuelsen, Phys. Rev. B **43**, 12799 (1991).
10. I.V.Vernik, S.Keil et al., submitted to Phys. Rev. B (May 1996).
11. A.A.Golubov, I.L.Serpuchenko and A.V.Ustinov. ZhETF **94**, 297 (1988) [Sov. Phys. JETP **67**, 1256 (1988)].